Research Square

Preprints are preliminary reports that have not undergone peer review.
They should not be considered conclusive, used to inform clinical practice,
or referenced by the media as validated information.

# Value of machine learning model based on superb microvascular imaging ultrasound radiomics in noninvasive assessment of chronic kidney disease

**Jiao Yao**
Sichuan University, Sichuan University affiliated Chengdu Second People's Hospital，Chengdu Second People's Hospital， Chengdu Second People's Hospital

**Jinfeng Qin**
Sichuan University, Sichuan University affiliated Chengdu Second People's Hospital，Chengdu Second People's Hospital， Chengdu Second People's Hospital

**Wei Yuan**
Sichuan University, Sichuan University affiliated Chengdu Second People's Hospital，Chengdu Second People's Hospital， Chengdu Second People's Hospital

**Wang Zhou**
First Affiliated Hospital of Anhui Medical University

**Xiachuan Qin**
11326636@qq.com

Sichuan University, Sichuan University affiliated Chengdu Second People's Hospital，Chengdu Second People's Hospital， Chengdu Second People's Hospital

**Article**

**Keywords:** chronic kidney disease, chronic degree, superb microvascular imaging, radiomics, machine learning, nomogram

**Posted Date:** November 19th, 2026

**DOI:** https://doi.org/10.21203/rs.3.rs-10666978/v1

**License:** This work is licensed under a Creative Commons Attribution 4.0 International License.
Read Full License

**Additional Declarations:** No competing interests reported.

# Abstract

To noninvasively assess the chronicity of chronic kidney disease (CKD) using a machine learning (ML) model based on superb microvascular imaging (SMI) ultrasound radiomics, and to develop and validate a clinical-radiomics nomogram for individualized prediction. A total of 305 patients with CKD confirmed by renal biopsy were prospectively enrolled and divided into training (n = 213) and test (n = 92) cohorts. Radiomic features were extracted from SMI ultrasound images of the renal cortex. The most valuable features were selected using univariate analysis, Spearman correlation analysis, and the least absolute shrinkage and selection operator (LASSO) algorithm. Five ML algorithms—logistic regression, random forest, support vector machine, k-nearest neighbor, and extreme gradient boosting (XGBoost)—were trained and compared. A clinical-radiomics nomogram was constructed by integrating the radiomics score (Rad-score) with independent clinical predictors. Model performance was evaluated using receiver operating characteristic (ROC) curves, calibration curves, and decision curve analysis (DCA). The XGBoost model demonstrated the best diagnostic performance among the five ML algorithms, with areas under the ROC curve (AUCs) of 0.903 and 0.888 in the training and test cohorts, respectively. Sex and estimated glomerular filtration rate (eGFR) were identified as independent clinical predictors. The combined clinical-radiomics nomogram, integrating the Rad-score with these clinical factors, showed excellent discrimination, with AUCs of 0.949 and 0.943 in the training and test cohorts, respectively. Calibration curves demonstrated good agreement between predicted and observed probabilities, and DCA confirmed the clinical utility of the nomogram. The ML classifier based on SMI ultrasound radiomics provides a promising noninvasive approach for assessing CKD chronicity. The nomogram combining SMI radiomic features with clinical characteristics offers clinicians comprehensive and personalized imaging information, which may facilitate individualized treatment decision-making.


# Introduction

Chronic kidney disease (CKD) is a very common disease and an important independent risk factor for adverse cardiovascular events such as coronary heart disease, stroke, and heart failure[1]. In 2017, 1.2 million people died of CKD worldwide, and CKD mortality increased by 41.5% between 1999 and 2017[2]. The sixth monitoring of chronic diseases and risk factors in China from 2018 to 2019 included CKD on the list of monitored diseases for the first time. Among 176,874 participants, the patient rate of CKD was as high as 8.2%, and a study reported that 82 million adults in China had CKD from 2018 to 2019[3]. Patients with CKD are the most complex and multi-disease patient group in internal medicine[4]. Considering the high incidence and latency characteristics of CKD, real-time monitoring of CKD progression is essential for the implementation of treatment, which can effectively prevent deterioration into severe renal dysfunction, such as end-stage renal disease (ESRD). Many studies have shown that chronic changes are powerful predictors of renal outcomes in various kidney diseases[5,6].Chronic changes involve the renal cortex and medulla, but they are most visible in the cortex, which can affect the glomeruli, renal tubules, interstitium, and arterioles. To accurately judge chronic changes in CKD, the 2017 International Society of Nephrology conducted overall chronic differentiation of the kidney

according to the results of renal biopsy (glomerulosclerosis, interstitial fibrosis, tubular pathology, and arteriosclerosis)[7]. Renal histopathology is considered the gold standard method for evaluating renal microstructure and quantifying the causes of renal dysfunction; however, the incidence of bleeding complications after renal biopsy as an invasive examination is 37.70%[8]. Invasive puncture is not suitable for long-term monitoring of disease progression or treatment response[9]; failure to know in time the degree of CKD in patients may lead to patients' inability to obtain the best treatment.

In the pathological process of CKD, renal microvascular changes such as intimal hyperplasia and intimal thickening decrease the lumen diameter, which in turn leads to an increase in the hemodynamic resistance of renal microvessels, and an increase in intrarenal vascular resistance leads to a decrease in renal cortical microvascular perfusion[10,11]. Therefore, renal blood flow imaging technology, which reflects the renal microvascular situation, may be a potential method for non-invasively assessing the chronicity of CKD. In recent years, superb microvascular imaging(SMI), a new noninvasive blood flow imaging mode, has been widely used in clinical practice. It uses a filter different from color doppler ultrasound（CDUS） to minimize motion artifacts and uses an adaptive calculation method to display real blood flow information. Even without the use of contrast agents, SMI can improve the visibility of low-speed blood flow and the sensitivity of small-vessel signal detection[12,13], Therefore, SMI shows great potential for displaying the micro blood flow of the kidney.

Radiomics transforms medical images into mineable high-throughput quantitative features[14,15], and the heterogeneity of lesions is evaluated using information related to the phenotype of lesions such as shape, intensity, wavelet, and texture. Recently, several studies have found that ultrasound radiomics can effectively identify biomarkers of subclinical changes in the kidneys based on ultrasound images[16,17]. Qin et al. extracted 1,314 ultrasound radiomic features from kidney ultrasound images. After screening, five ultrasound radiomics features were retained. The XGBoost model was used to noninvasively diagnose the chronicity of lupus nephropathy. The AUC of the ROC curve for the test group was 0.826[18]. Qin et al. extracted the radiomic features of ultrasound images of patients with IgAN to establish a machine learning (ML) model and attempted to noninvasively diagnose whether there was a crescent in IgAN. The test group obtained the best results with an accuracy of 72.8%[17]. These results demonstrate that the ultrasound radiomics model has a strong ability to process high-throughput data. Although many internal details of the image are not recognized by the naked eye of the sonographer, they can be obtained using ultrasound radiomics[19,20]. To the best of our knowledge, no studies have used a radiomics ML model of SMI to noninvasively assess the chronicity of CKD. Therefore, this study aimed to develop and validate a nomogram model that combines an ML model based on SMI image radiomics with clinical factors for the personalized noninvasive assessment of chronicity in patients with CKD.

# Methods

This study conformed to the ethical guidelines of the Declaration of Helsinki and was approved by the Ethics Committee of Chengdu Second People's Hospital. Written informed consent was obtained from

all patient participants. This prospective study consecutively enrolled 305 patients with CKD who underwent renal biopsy at two independent medical centers (Chengdu Second People's Hospital, Chengdu, China; and The First Affiliated Hospital of Anhui Medical University, Hefei, China) between June 2022 and October 2023.

The inclusion criteria were as follows: 1. more than 10 glomeruli in light microscopy specimens, 2. being older than 18 years, and 3. the distance between the kidney and the skin was less than 5 cm. The exclusion criteria were: 1. acute kidney injury and heart valve disease, 2. urinary tract obstruction, 3. cysts or tumors in the kidneys, and 4. Doppler patterns suggestive of renal artery stenosis[21]. After screening, 305 patients were included in the study and divided into training and test groups at a ratio of 7:3. A research flowchart is shown in Fig. 1.

# Renal biopsy and pathological grading

Renal biopsy was performed within 3 days of renal CDUS measurement, with the cooperation of an experienced nephrologist and an ultrasound interventional physician as part of their routine clinical duties. All renal puncture tissues were examined by electron and light microscopy. All biopsy samples contained at least 10 glomeruli. Glomerulosclerosis, tubular atrophy, and interstitial fibrosis scores ranged from 0 to 3 (the rates of tissue compartment involvement were < 10%, 10–25%, 26–50%, and > 50%, respectively). When the intimal thickness was 0, the arteriosclerosis score was 0 or less than the medial thickness; otherwise, it was recorded as 1. The total CKD score of chronic kidney disease was calculated by summing up the scores. The overall severity of chronic kidney disease in CKD was divided into minimal (total score of 0–1), mild (total score of 2–4), moderate (total score of 5–7), and severe (total score ≥ 8) [7]. Furthermore, we divided the minimal/mild and moderate-to-severe groups into two groups.

## Ultrasonic image collection

Three experienced ultrasound diagnosticians (with 6, 10, and 16 years of experience in abdominal ultrasound examination) collected ultrasound and SMI images using a Canon ultrasound diagnostic instrument (Aplio i700; Canon Medical Systems, Otawara, Japan) equipped with a 3.5 MHz convex array probe (i8c1).

The patient fasted for > 8 h before the ultrasound examination. The patient was placed in the lateral position. During ultrasound examination, the patient was instructed to pause breathing at the end of inspiration. The ultrasound probe was gently positioned in the flank in the form of an oblique projection, and a 3.5 MHz probe was used for ultrasound examination of the target kidney. The probe was placed on the posterior axillary line, and its position and angle were adjusted to obtain a maximum longitudinal ultrasound image of the target kidney. After the maximum longitudinal section of the kidney was obtained, the settings of the ultrasound diagnostic instrument were switched to color SMI mode, and the

specific area of interest box of SMI was placed on the whole kidney to obtain the optimal blood flow section of the kidney.

## Establishment of clinical model

We collected the color Doppler ultrasound parameters and clinical data of the patients three days before puncture (see Supplementary Material). First, univariate logistic regression analysis was used to analyze the association between the traditional color Doppler ultrasound parameters and the chronicity of CKD; then, the related factors ($P < 0.1$) obtained from the above univariate regression analysis were subjected to multivariate logistic regression analysis to determine the independent predictive factors significantly related to the chronicity of CKD and to establish the clinical diagnosis model.

## Machine learning model of ultrasound radiomics

The ultrasound images of all patients were directly exported and stored in the ultrasound diagnostic instrument in digital imaging and communication in medicine (DICOM) format. First, we imported the target kidney ultrasound and SMI images into ITK-SNAP medical image segmentation software (version 3.8.0, http://www.itksnap.org/pmwiki/pmwiki.php?n=Downloads.SNAP3). The maximum longitudinal section of the target kidney was selected, and the target renal cortex was annotated as the region of interest (ROI). Figure 2 shows the workflow of the SMI-based ultrasound radiomics model. The ultrasound images of 50 patients were randomly selected, and ROI segmentation was performed by two ultrasound doctors, one with 10 years of abdominal ultrasound experience and another with 8 years of abdominal ultrasound experience, who were blinded to the results. Intraclass and intergroup correlation coefficients (ICC) were used to evaluate the consistency of characteristics between groups. After two weeks, sonographer 1 repeated the same steps to evaluate the intragroup consistency of feature extraction. When the ICC value is greater than or equal to 0.75, it indicates that the extracted features have good consistency, and features with $ICC < 0.75$ are removed in the subsequent analysis. The remaining image segmentation was performed using Ultrasound Doctor 1.

Radiomics feature extraction was performed using pyradiomics in python (version 2.2.0, http://www.radiomics.io/pyradiomics.htm). It can extract features from ultrasonic images by using coding feature algorithm. The extracted features included the original image, wavelet, square, square root, logarithm, exponent, gradient, and local binary-mode 2D and 3D filters. The steps of selecting sonoradiomics features were as follows. First, the features with $ICC > 0.75$ in the training cohort were retained. Second, the univariate rank sum test was used to screen the statistically significant differences between the minimum/mild group and the moderate/severe group in the training cohort. Subsequently, the normality of the remaining radiomics features was tested. Pearson correlation analysis was used for the features that conform to the normal distribution, and Spearman correlation analysis was used for the features that do not conform to the normal distribution; redundant features with correlation coefficient >

0.80 were removed. Fourth, an elastic network regression algorithm was performed on the radiomics features[22]. Analyze and select the most valuable features.

We trained five ML algorithms based on the radiomics feature selection results, including logistic regression (LR), random forest (RF), support vector machine (SVM), k-nearest neighbor (KNN), and extreme gradient boosting (XGBoost). The grid search method and ten- fold cross validation of the training dataset were used for the adjustment. In each cycle, the hyperparameters with the highest AUC in the training group were retained.

## Establishment of nomogram combination model

We used clinically independent predictors obtained in the training cohort and the optimal rad score of ML, a model that integrates radiomics and clinical features based on SMI images. The discriminative performance of the model was evaluated using receiver operating characteristic (ROC) curve analysis, whereas the goodness of fit was evaluated using calibration curves. Decision curve analysis (DCA) was performed to evaluate the clinical utility of the model.

# Statistical analysis

SPSS 26.0 (IBM Corp., Armonk, NY, USA) and Python 2.7 (Python Software Foundation, Beaverton, USA) were used for all statistical analyses. Quantitative data with normal distribution are expressed as mean ± standard deviation, while quantitative data without normal distribution are expressed as median ± interquartile range. Categorical variables were expressed as numbers and percentages. The chi-square test, two independent samples t-test, and Mann–Whitney U test were used for univariate analysis. Statistical significance was set at $P < 0.05$.

## Results

# General clinical characteristics of patients

A total of 305 patients with CKD and undergoing renal biopsy were recruited in this study, including 153 males and 152 females, aged 43 ± 13 (range, 18–76 years). A total of 202 patients had minimal/mild CKD and 103 patients had moderate-to-severe CKD. There were 213 patients in the training group, 107 males and 106 females and aged 41.8 ± 12.9 (18–75 years), including 144 patients with minimal/mild CKD and 72 patients with moderate-to-severe CKD. There were 92 patients in the test group, 46 males and 46 females and aged 45.7 ± 13 (21–76 years), including 68 patients with minimal/mild CKD and 31 patients with moderate-to-severe CKD. The clinical basic characteristics of patients with CKD are shown in Table 1.

Table 1
Clinical factors in the training and testing group

| **Sex(male/female)** | **Training group** | **Testing group** |
|---|---|---|
| | **107/106** | **46/46** |
| Age (years) | 41.8 ± 12.9 | 45.7 ± 13 |
| Creatinine(umol/L) | 100.3 ± 77.1 | 92.1 ± 34.8 |
| eGFR (mL/min/1.73m$^2$) | 90.1 ± 33.8 | 86.5 ± 25.7 |
| UA(umol/L) | 372.7 ± 99.1 | 378.3 ± 112.1 |
| UREA(mmol/L) | 6.4 ± 3.14 | 6.6 ± 2.69 |
| 24-hour proteinuria (g/24h) | 2.6 ± 3.38 | 2.6 ± 3.51 |
| Renal length(mm) | 106 ± 8.5 | 105.3 ± 9.2 |
| Renal cortical thickness(mm) | 7.7 ± 1.2 | 7.7 ± 1.1 |
| Renal artery resistance index | 0.67 ± 0.06 | 0.67 ± 0.06 |
| GS (0/1/2/3) | 77/98/35/3 | 36/40/13/3 |
| IF (0/1/2/3) | 82/68/61/2 | 37/26/25/4 |
| TA (0/1/2/3) | 82/69/61/1 | 37/26/26/3 |
| CV (0/1) | 54/159 | 24/68 |

# Diagnostic performance of clinical models

Univariate and multivariate regression analyses showed that sex (p = 0.01) and eGFR (p = 0.001) were independent predictors of CKD chronicity in the clinical model (Supplementary Material).

In the training group, the AUC of the ROC curve for the clinical model was 0.859 (0.805–0.913), with an accuracy of 0.826, sensitivity of 0.722, specificity of 0.879, PPV of 0.754, and NPV of 0.861. In the test group, the AUC of the ROC curve of the clinical model was 0.887 (0.812–0.963), with an accuracy of 0.837, sensitivity of 0.806, specificity of 0.852, positive PPV value of 0.735, and negative predictive value of 0.897.

# Diagnostic performance of the ultrasound radiomics model

A total of 1,746 ultrasound radiomics features were extracted from the ultrasound images. After inter- and intra-observer analyses and univariate correlation analysis, 1,325 ultrasound radiomics characteristics showed significant differences between the two groups. After the significance analysis of radiomics features using the single factor rank sum test, 530 related features were obtained, and Spearman correlation analysis was performed on the radiomics features and the remaining 28 radiomics

features. Finally, elastic logistic analysis was performed to generate the 13 most valuable ultrasound radiomics features [log (λ) = − 2.808, = 0.5](Table 2)

Table 2
Coefficients of Selected Features in the Ultrasound Radiomics Model

| Features | Coefficient | OR |
|---|---|---|
| SMI_wavelet.LHL_glszm_GrayLevelNonUniformity | -0.26197 | 0.769532 |
| SMI_wavelet.LLH_firstorder_RootMeanSquared | -0.1994 | 0.819226 |
| US_wavelet.HHH_glszm_SizeZoneNonUniformityNormalized | -0.14052 | 0.868909 |
| US_wavelet.LLL_glrlm_RunVariance | -0.12923 | 0.87877 |
| SMI_wavelet.HLH_glszm_LowGrayLevelZoneEmphasis | -0.07651 | 0.926345 |
| SMI_wavelet.LLH_gldm_LargeDependenceLowGrayLevelEmphasis | -0.07621 | 0.926618 |
| SMI_wavelet.HHL_firstorder_RobustMeanAbsoluteDeviation | -0.04071 | 0.960112 |
| SMI_wavelet.LLL_glrlm_RunVariance | -0.0153 | 0.984813 |
| SMI_wavelet.LHL_glszm_SizeZoneNonUniformityNormalized | -0.0105 | 0.989559 |
| SMI_wavelet.HLL_glszm_GrayLevelNonUniformity | -0.00707 | 0.992957 |
| US_wavelet.LLL_firstorder_Minimum | 0.068774 | 1.071194 |
| SMI_wavelet.HLL_firstorder_RootMeanSquared | 0.095141 | 1.099814 |
| US_wavelet.LHH_glrlm_RunLengthNonUniformityNormalized | 0.12807 | 1.136633 |

We constructed five different ML models using different algorithms. The diagnostic performances of these ML models are listed in Table 3. The ROC and DCA curves of the five models based on the training and test groups are shown in Fig. 3. The diagnostic efficiency of the XGBoost model was the best for judging the chronicity of CKD. The AUC of the training group was 0.903 (0.861–0.946), with an accuracy rate of 0.798, sensitivity of 0.944, specificity of 0.723, PPV of 0.636, and NPV of 0.962. The AUC of the test group was 0.888 (0.82–0.957), with an accuracy rate of 0.815, sensitivity of 0.903, specificity of 0.77, PPV of 0.667, and NPV of 0.94. At the same time, in the training and test groups, the DCA curve proves that XGBoost has a higher overall net benefit than the other four ML models.

Table 3
Performance of five radiomics models in the training and the testing group

| Train | Model | AUC (95% CI) | ACC | SEN | SPE | PPV | NPV |
|---|---|---|---|---|---|---|---|
| | **SVM** | **0.701 (0.64–0.762)** | **0.681** | **0.722** | **0.638** | **0.671** | **0.692** |
| | RF | 0.849 (0.806–0.892) | 0.768 | 0.708 | 0.83 | 0.81 | 0.736 |
| | DT | 0.858 (0.817–0.899) | 0.788 | 0.778 | 0.801 | 0.8 | 0.779 |
| | KNN | 0.716 (0.657–0.775) | 0.677 | 0.694 | 0.66 | 0.676 | 0.679 |
| | Xgboost | 0.903 (0.861–0.946) | 0.798 | 0.944 | 0.723 | 0.636 | 0.962 |
| Test | SVM | 0.811 (0.724–0.898) | 0.772 | 0.742 | 0.787 | 0.639 | 0.857 |
| | RF | 0.845 (0.754–0.936) | 0.815 | 0.806 | 0.82 | 0.694 | 0.893 |
| | DT | 0.783 (0.672–0.895) | 0.75 | 0.71 | 0.77 | 0.611 | 0.839 |
| | KNN | 0.709 (0.594–0.825) | 0.728 | 0.548 | 0.82 | 0.607 | 0.781 |
| | Xgboost | 0.888 (0.82–0.957) | 0.815 | 0.903 | 0.77 | 0.667 | 0.94 |

# Clinical sonomics nomogram

By combining the radscore and clinical characteristics(Figure 4), the AUC of establishing clinical sonomics nomogram based on the training cohort of 213 patients was 0.949 (0.92–0.978), with an accuracy of 0.911, specificity of 0.901, sensitivity of 0.931, ppv of 0.827, and NPV of 0.962. In the test group, the AUC was 0.943 (0.88–0.99), with an accuracy of 0.913, specificity of 0.984, and sensitivity of 0.774. The PPV and NPV was 0.96 and 0.896, respectively. The calibration curve of the combined model showed good agreement between the predicted and observed values in the training and test sets. The discriminant efficacies of the three diagnostic models (clinical, ultrasound radiomics, and clinical ultrasound radiomics) are shown in Table 4. The ROC curves of the three models based on the training and test groups are shown in Fig. 5. Decision curve analysis was used to demonstrate the clinical decision utility of the combined model, showing the corresponding clinical utility of the strategy.

Table 4
Performance of the clinical model, radiomics model, and combined nomogram in the training and testing cohorts

| Model | AUC (95% CI) | ACC | SEN | SPE | PPV | NPV |
|---|---|---|---|---|---|---|
| **Training group** | | | | | | |
| Clinical | 0.859 (0.805–0.913) | 0.826 | 0.722 | 0.879 | 0.754 | 0.861 |
| Radiomics | 0.903 (0.861–0.946) | 0.798 | 0.944 | 0.723 | 0.636 | 0.962 |
| Nomogram | 0.949 (0.92–0.978) | 0.911 | 0.931 | 0.901 | 0.827 | 0.962 |
| **Testing group** | | | | | | |
| Clinical | 0.887 (0.812–0.963) | 0.837 | 0.806 | 0.852 | 0.735 | 0.897 |
| Radiomics | 0.888 (0.82–0.957) | 0.815 | 0.903 | 0.77 | 0.667 | 0.94 |
| Nomogram | 0.943 (0.88–0.99) | 0.913 | 0.774 | 0.984 | 0.96 | 0.896 |
| AUC=Area under the curve; ACC=Accuracy;SEN=Sensitivity; SPE=Specificity; | | | | | | |
| NPV = Negative predictive value, PPV = Positive predictive value | | | | | | |

# Discussion

Pathological damage caused by CKD is complex and variable. Several studies have shown that renal pathologists believe that glomerulosclerosis, tubular atrophy, interstitial fibrosis, and arteriosclerosis in renal biopsies are prognostic indicators of CKD progression using semiquantitative scoring[5,23]. However, the determination of the degree of chronic disease is based on renal biopsy. Renal biopsies are invasive, carry the risk of sampling errors, and provide limited spatial information. It is not suitable for long-term monitoring of disease progression or evaluation of treatment responses. Therefore, a precise and noninvasive method is required. In this study, we selected 13 ultrasound radiomics features from kidney ultrasound SMI images to determine the chronicity of CKD nephropathy. These radiomics features are used to build a prediction model using various classical classification algorithms. Among them, the XGBoost classifier had the best comprehensive performance in the noninvasive evaluation of chronicity, and the AUCs of the training and test groups were as high as 0.903 and 0.888, respectively. This indicates that machine learning has strong processing ability for high-throughput data. To our knowledge, this is the first study to noninvasively detect the chronic degree of CKD based on machine learning model analysis of the radiomics features of SMI ultrasound images. However, the nomogram of clinical ultrasound radiomics can further improve its prediction efficiency, and the ROC of the training and testing groups were as high as 0.949 and 0.943, respectively.

Several baseline clinical data points were analyzed. Univariate and multivariate logistic regression analyses showed that sex and eGFR status were independent predictors in the clinical model. It is generally believed that male patients are more likely than women to develop ESRD because of their

unhealthy lifestyle [24,25]. True glomerular filtration rate (GFR) cannot be directly measured in humans. The GFR can be assessed by the clearance of filtration markers (low-molecular-weight substances eliminated mainly by glomerular filtration) or plasma (or serum) concentration, which is currently the clearest characteristic indicator used to reflect the chronicity of the kidney[26,27]. We established a clinical model based on sex and eGFR to noninvasively assess the degree of chronic CKD and obtained results for the training and test groups. However, the accuracy of the eGFR is affected by non-GFR determinations of the filtration marker[26,28]. At the same time, some methods that more accurately reflect the real pathology are needed. Renal perfusion is abundant and highly vascularized, and renal blood flow usually accounts for 25% of cardiac output[29].

In the process of kidney chronicity, renal microvascular changes, such as gradual proliferation and thickening of the inner membrane of small renal vessels, lead to a reduction in the lumen diameter and an increase in renal microvascular resistance. An increase in intrarenal vascular resistance leads to a decrease in renal cortical microvascular perfusion[11]. Zhang used CDUS to grade the renal blood flow distribution of IgAN and found that the degree of reduction in renal blood flow distribution was closely related to the degree of renal chronicity[30]. We chose SMI to evaluate the chronicity of CKD because it is superior to CDUS and PDUs in delineating the Renal Cortical Microvasculature[31]. Features that can be observed in the kidney by the human eye are limited, and many internal details of the image are unrecognizable to the naked eye. Compared to traditional diagnostic imaging, ultrasound radiomics can extract the micro-features of ROI in medical images and convert medical images related to lesion pathophysiology information into high-dimensional data that can be mined[19]. In this study, we extracted 1,746 ultrasound radiomic features from ultrasound and SMI images. After data dimensionality reduction analysis, we obtained 13 ultrasound radiomics features highly related to those of patients with CKD, including four ultrasound and nine SMI features. These texture features reflect microscopic features that cannot be recognized by the human eye in ultrasound images. Furthermore, we established five ML diagnostic models based on these 13 ultrasound radiomics features. Among them, the XGBoost model obtained the best results, and the AUC of the ROC curve in the validation and test groups were 0.903 and 0.888, respectively, which were better than those of the clinical model based on eGFR.

The nomogram model is a graphic ruler widely used in the medical field. It combines the important parameters of logistic regression analysis to generate a single numerical probability for the relevant variables of the prediction results and creates a friendly and understandable image interface to help clinicians calculate the risks of different conditions to carry out personalized decision analysis[32]. Therefore, we developed a practical nomogram that integrates the proposed clinical data, ultrasound characteristics, and radiomics scores to accurately personalize the prediction of CKD chronicity. In this study, the radiomics nomogram constructed using eGFR and RS achieved good calibration and satisfactory discrimination (the ROC of the training and test groups was 0.949 and 0.943, respectively), and the results were better than those of the single radiomics and clinical models. According to this model, we can effectively obtain the personalized degree of kidney chronicity for each patient with CKD. Therefore, nomograms can be used as reliable non-invasive tools and can help clinicians choose

personalized treatment strategies. To our knowledge, this is the first study to diagnose the chronicity of CKD based on a clinical SMI radiomics nomogram model.

Our study has some limitations. First, some statistical deviations are inevitable in studies of a single race. It is therefore necessary to conduct multi-ethnic validation to obtain high-level evidence for further clinical applications. Second, due to the limitation of sample size, only the minimum mild and moderately severe groups could be grouped for comparison. In future research, we will expand on these cases and refine the differentiation of all subgroups.

In conclusion, this study developed a clinical ultrasound radiomics nomogram based on clinical and SMI radiomics features, which has high discrimination accuracy in the noninvasive diagnosis of chronic CKD nephropathy, provides doctors with more comprehensive and personalized image information, and is of great significance for clinical doctors to choose treatment strategies.

## Declarations

**Subject terms:** Nephrology, Ultrasound Imaging, Radiomics, Machine Learning, Medical Image Processing, Clinical Prediction Models, Noninvasive Diagnosis

# Competing interests

The authors declare no competing interests.

# Funding

This study has received funding from the Chengdu Medical Research Project (Item No. 2025056).

# Author Contribution

J Y: Software, Visualization, Data curation, Methodology, Formal analysis, Writing – original draft, Conceptualization. Jf Q, W Y: Formal analysis, Software, Visualization, Resources, Conceptualization . W Z, Xc Q: review , editing, Investigation, Supervision, Validation.

# Acknowledgment

No.

# Data Availability

The datasets generated during and/or analysed during the current study are available from the corresponding author on reasonable request.

## References


1. Buckley, L. F. et al. Associations Between Kidney Histopathologic Lesions and Incident Cardiovascular Disease in Adults With Chronic Kidney Disease. *JAMA Cardiol.* **8** (4), 357–365 (2023).
2. Global & national burden of chronic kidney disease. 1990–2017: a systematic analysis for the Global Burden of Disease Study 2017. *Lancet (London England)*. **395** (10225), 709–733 (2020).
3. Wang, L. et al. Prevalence of Chronic Kidney Disease in China: Results From the Sixth China Chronic Disease and Risk Factor Surveillance. *JAMA Intern. Med.* **183** (4), 298–310 (2023).
4. Klinkhammer, B. M. & Boor, P. Kidney fibrosis: Emerging diagnostic and therapeutic strategies. *Mol. Aspects Med.* **93**, 101206 (2023).
5. Denic, A. et al. Prognostic Implications of a Morphometric Evaluation for Chronic Changes on All Diagnostic Native Kidney Biopsies. *J. Am. Soc. Nephrology: JASN*. **33** (10), 1927–1941 (2022).
6. Ren, W. et al. Significance of the total renal chronicity score in predicting renal outcome in PLA2R-associated membranous nephropathy. *Journal nephrology* (2024).
7. Sethi, S. et al. A proposal for standardized grading of chronic changes in native kidney biopsy specimens. *Kidney Int.* **91** (4), 787–789 (2017).
8. Li, F. F. et al. Analysis of hemorrhage upon ultrasound-guided percutaneous renal biopsy in China: a retrospective study. *International Urol. nephrology* (2023).
9. Hogan, J. J., Mocanu, M. & Berns, J. S. The Native Kidney Biopsy: Update and Evidence for Best Practice. *Clin. J. Am. Soc. Nephrology: CJASN*. **11** (2), 354–362 (2016).
10. Fischer, K. et al. High-resolution renal perfusion mapping using contrast-enhanced ultrasonography in ischemia-reperfusion injury monitors changes in renal microperfusion. *Kidney Int.* **89** (6), 1388–1398 (2016).
11. Levin, A. & Stevens, L. A. Executing change in the management of chronic kidney disease: perspectives on guidelines and practice. *Med. Clin. North. Am.* **89** (3), 701–709 (2005).
12. Collaku, E. et al. Superb Microvascular Imaging (SMI) Compared with Color Doppler Ultrasound for the Assessment of Hepatic Artery in Pediatric Liver Transplants: A Feasibility Study. *Diagnostics (Basel Switzerland)* ;**12**(6). (2022).
13. Jeon, S. K., Lee, J. Y., Kang, H. J. & Han, J. K. Additional value of superb microvascular imaging of ultrasound examinations to evaluate focal liver lesions. *Eur. J. Radiol.* **152**, 110332 (2022).
14. Lambin, P. et al. Radiomics: the bridge between medical imaging and personalized medicine. *Nat. Rev. Clin. Oncol.* **14** (12), 749–762 (2017).
15. Bi, W. L. et al. Artificial intelligence in cancer imaging: Clinical challenges and applications. *Cancer J. Clin.* **69** (2), 127–157 (2019).

16. Qin, X. et al. Noninvasive Evaluation of Lupus Nephritis Activity Using a Radiomics Machine Learning Model Based on Ultrasound. *J. Inflamm. Res.* **16**, 433–441 (2023).
17. Qin, X. et al. A novel clinical-radiomic nomogram for the crescent status in IgA nephropathy. *Front. Endocrinol.* **14**, 1093452 (2023).
18. Yin, C. et al. Non-invasive prediction of the chronic degree of lupus nephropathy based on ultrasound radiomics. *Lupus* **33** (2), 121–128 (2024).
19. Gillies, R. J., Kinahan, P. E. & Hricak, H. Radiomics: Images Are More than Pictures, They Are Data. *Radiology* **278** (2), 563–577 (2016).
20. Bera, K., Braman, N., Gupta, A., Velcheti, V. & Madabhushi, A. Predicting cancer outcomes with radiomics and artificial intelligence in radiology. *Nat. Rev. Clin. Oncol.* **19** (2), 132–146 (2022).
21. Kliewer, M. A. et al. Renal artery stenosis: analysis of Doppler waveform parameters and tardus-parvus pattern. *Radiology* **189** (3), 779–787 (1993).
22. Zou, H. *Some perspectives of sparse statistical modeling* (Stanford University, 2005).
23. Eadon, M. T. et al. Kidney Histopathology and Prediction of Kidney Failure: A Retrospective Cohort Study. *Am. J. kidney diseases: official J. Natl. Kidney Foundation*. **76** (3), 350–360 (2020).
24. Wen, D. et al. Sex disparities in IgA nephropathy: a retrospective study in Chinese patients. *Int. Urol. Nephrol.* **53** (2), 315–323 (2021).
25. Huang, P. P. et al. Association between lifestyle, gender and risk for developing end-stage renal failure in IgA nephropathy: a case-control study within 10 years. *Ren. Fail.* **41** (1), 914–920 (2019).
26. Levey, A. S., Grams, M. E. & Inker, L. A. Uses of GFR and Albuminuria Level in Acute and Chronic Kidney Disease. *N. Engl. J. Med.* **386** (22), 2120–2128 (2022).
27. Inker, L. A. et al. Clinical Trial Considerations in Developing Treatments for Early Stages of Common, Chronic Kidney Diseases: A Scientific Workshop Cosponsored by the National Kidney Foundation and the US Food and Drug Administration. *Am. J. kidney diseases: official J. Natl. Kidney Foundation*. **80** (4), 513–526 (2022).
28. Levey, A. S., Coresh, J., Tighiouart, H., Greene, T. & Inker, L. A. Measured and estimated glomerular filtration rate: current status and future directions. *Nat. Rev. Nephrol.* **16** (1), 51–64 (2020).
29. Carlström, M., Wilcox, C. S. & Arendshorst, W. J. Renal autoregulation in health and disease. *Physiol. Rev.* **95** (2), 405–511 (2015).
30. Zhang, J. et al. Color Doppler Ultrasound and Hemodynamics for Evaluating Graft Dysfunction in Recurrent Immunoglobulin A Nephropathy. *Ann. Transplant.* **26**, e931736 (2021).
31. Gürbüz, A. F. et al. A comparison between the superb microvascular imaging technique and conventional Doppler ultrasound in evaluating chronic allograft damage in renal transplant recipients. *Diagn. Interv Radiol.* **29** (2), 212–218 (2023).
32. Fu, A. Z., Cantor, S. B. & Kattan, M. W. Use of nomograms for personalized decision-analytic recommendations. *Med. Decis. Mak.* **30** (2), 267–274 (2010).

# Figures

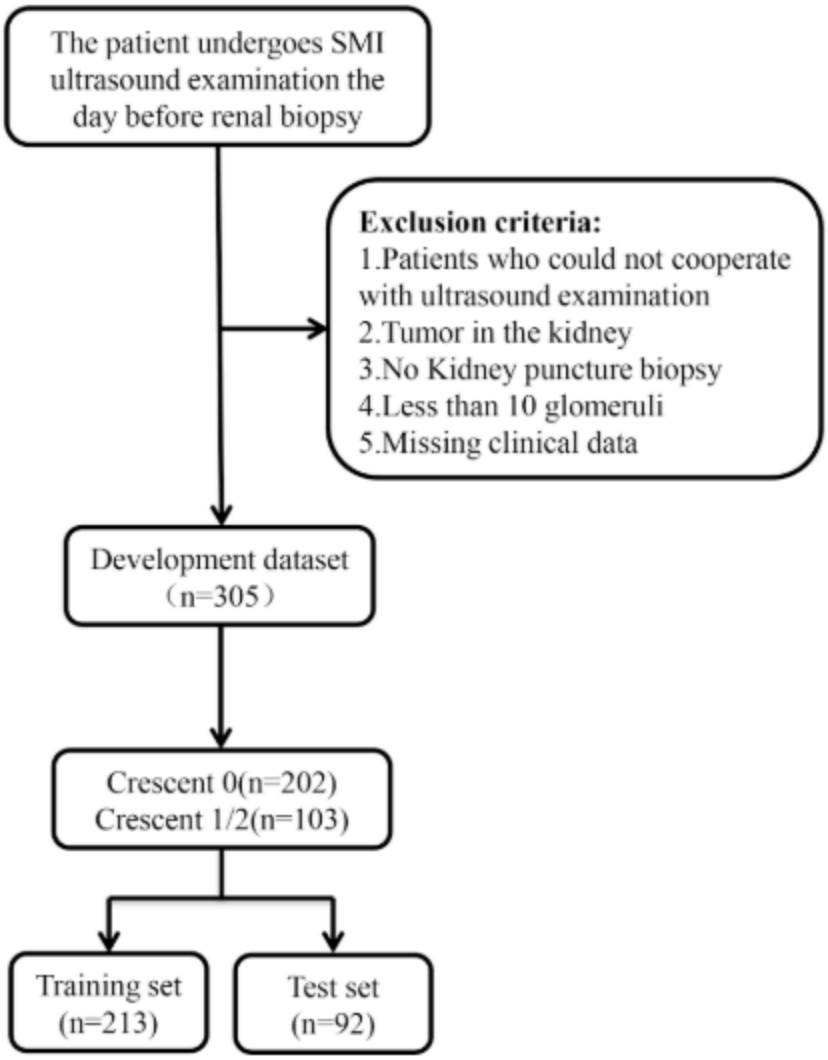



**Figure 1**

Patient flowchart

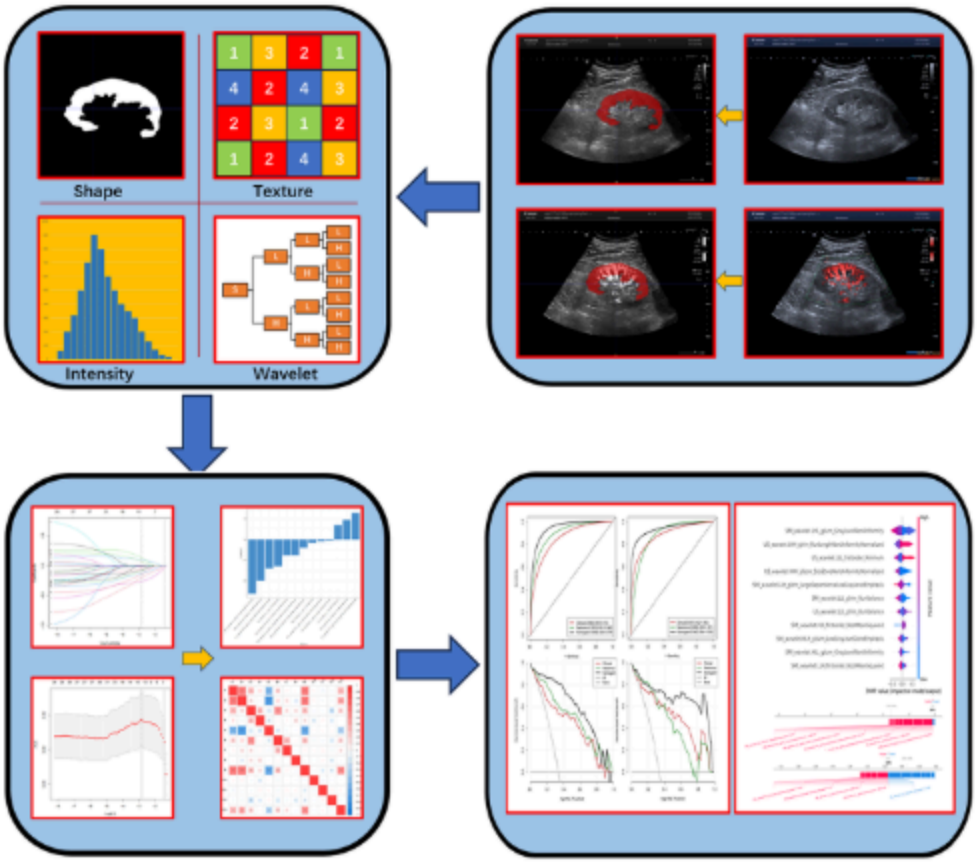



**Figure 2**

The ultrasound radiomics flow chart of the study.

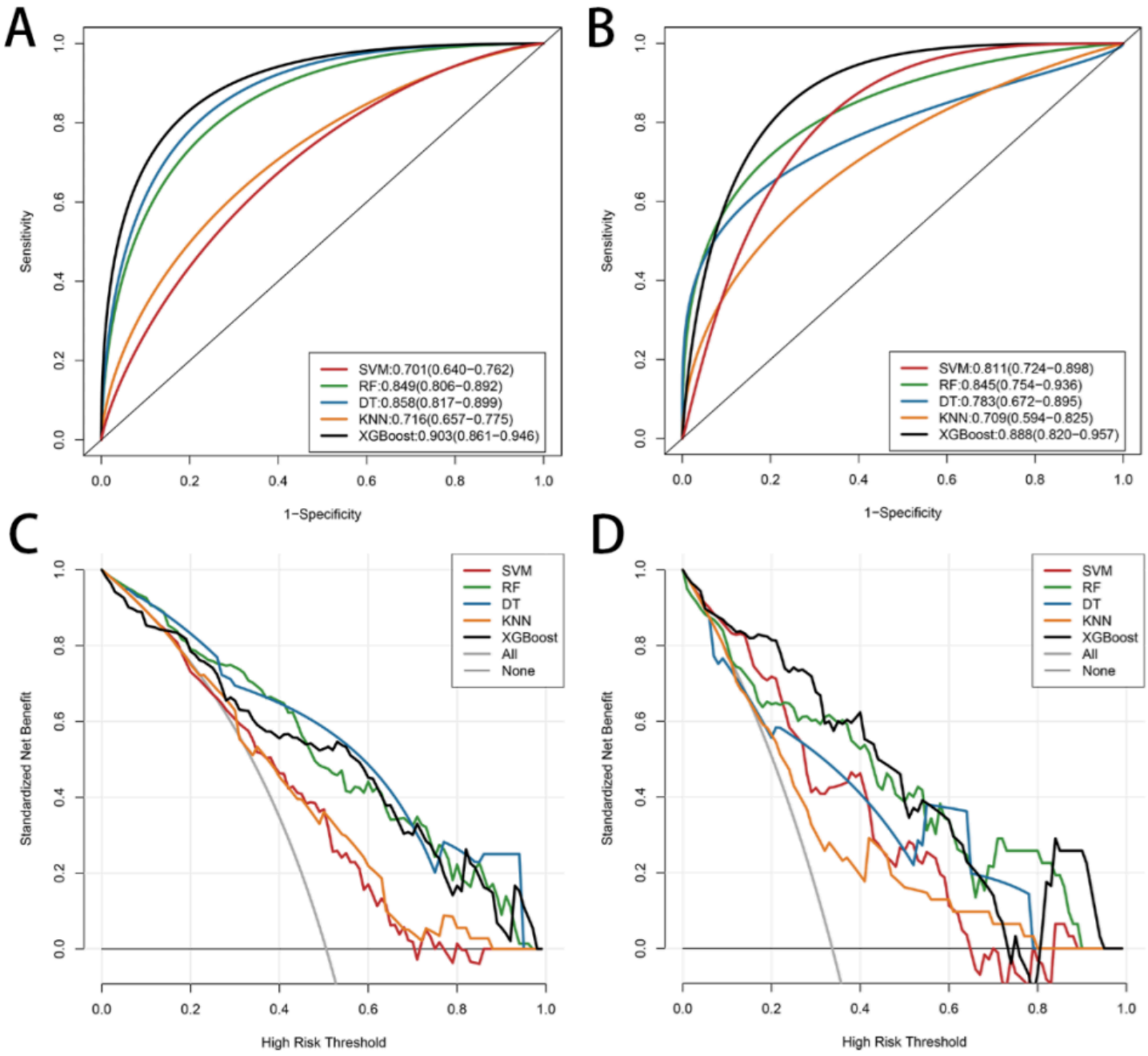



**Figure 3**

ROC and DCA curves of five machine learning (ML) models.A and D show the ROC and DCA curves of the five ML models in the training group. B and E represent the ROC and DCA curves of five ML models in the validation group.

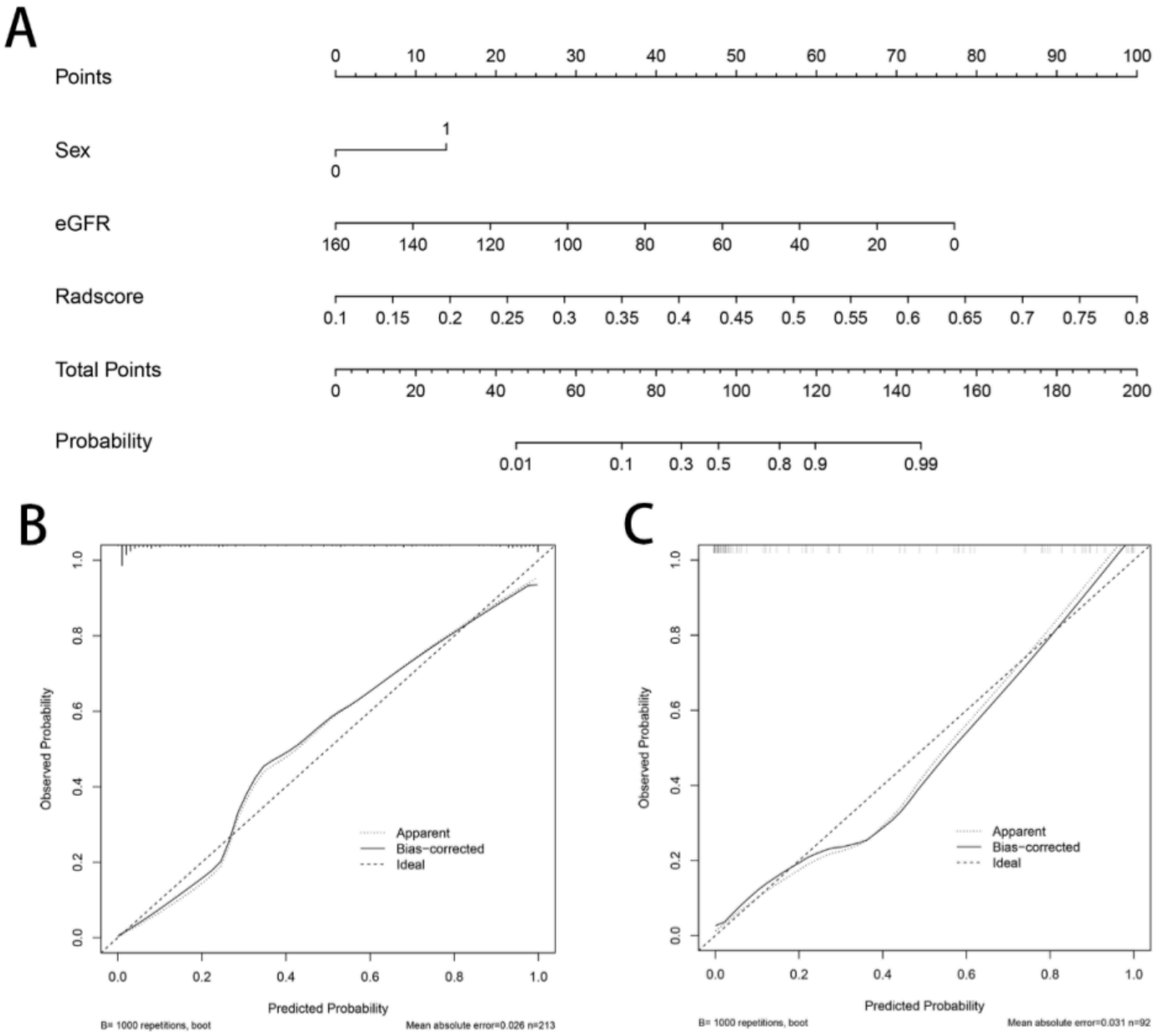



**Figure 4**

Performance of the combined clinical-radiomics nomogram.A.The clinical radiomics nomogram.The values of clinical characteristics and radscore can be converted into quantitative values according to the points axis.After summing the individual points to achieve the final sum shown on the total points axis,The evaluation of this chronicity is shown;B.The calibration plot also showed good agreement between the transition probabilities predicted by the nomogram in the training cohort; C.The calibration plot also showed good agreement in the testing cohort.

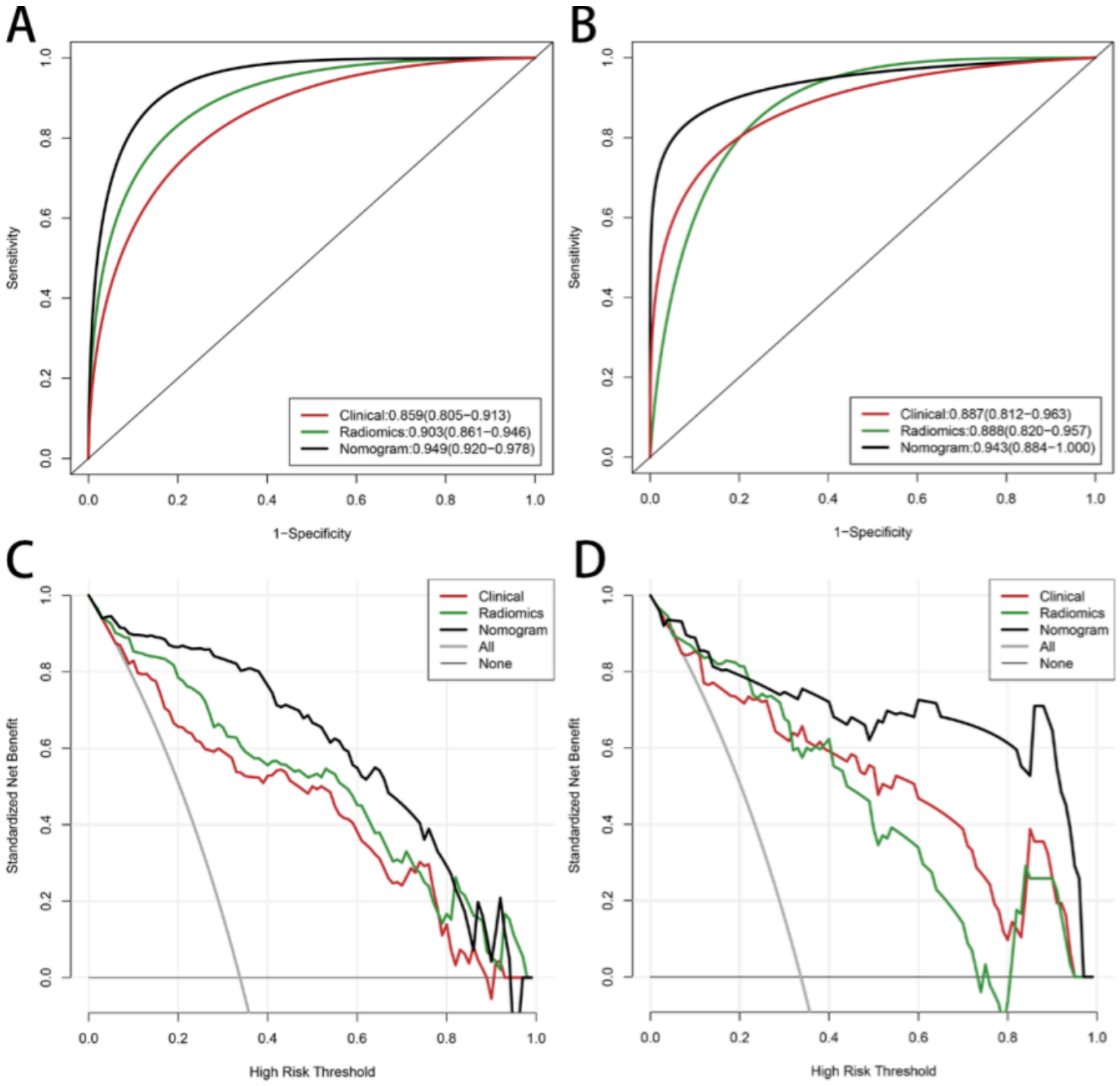



**Figure 5**

ROC and DCA curves of three prediction models. A and D show the ROC and DCA curves of the 3 models in the training group. B and E represent the ROC and DCA curves of 3 models in the validation group.

## Supplementary Files

This is a list of supplementary files associated with this preprint. Click to download.

- SupplementaryMaterial.pdf